1-4-2006

Simulation of HTS saturable core-type FCLs for MV distribution systems

S B. Abbott
University of Wollongong

Duane Robinson
University of Wollongong, duane@uow.edu.au

S Perera
University of Wollongong, sarath@uow.edu.au

F A. Darmann
Australian Superconductors, Port Kembla

C J. Hawley
University of Wollongong, hawley@uow.edu.au

See next page for additional authors

Simulation of HTS saturable core-type FCLs for MV distribution systems

Abstract

The design principles and performance characteristics of a prototype high-temperature superconductor saturable magnetic core-type fault current limiter are described. These are based on a distribution network service provider feasibility specification that included the footprint and regulatory requirements for limiting fault currents. Time-domain simulations using PSCAD/EMTDC are given to illustrate specific applications and the transient behavior of the different distribution system configurations are investigated.

Publication Details

This article was originally published as: Abbott, SB, Robinson, DA, Perera, S, et al, Simulation of HTS saturable core-type FCLs for MV distribution systems, IEEE Transactions on Power Delivery, April 2006, 21(2), 1013-1018. Copyright 2006 IEEE.

Authors

S B. Abbott, Duane Robinson, S Perera, F A. Darmann, C J. Hawley, and T P. Beales

Simulation of HTS Saturable Core-Type FCLs for MV Distribution Systems

S. B. Abbott, *Member, IEEE*, D. A. Robinson, S. Perera, *Member, IEEE*, F. A. Darmann, C. J. Hawley, and T. P. Beales

***Abstract*—The design principles and performance characteristics of a prototype high-temperature superconductor saturable magnetic core-type fault current limiter are described. These are based on a distribution network service provider feasibility specification that included the footprint and regulatory requirements for limiting fault currents. Time-domain simulations using PSCAD/EMTDC are given to illustrate specific applications and the transient behavior of the different distribution system configurations are investigated.**

***Index Terms*—Distribution, fault current limiter (FCL), high-temperature superconductor (HTS), saturable magnetic core, substation, superconductor.**

I. Introduction

INCREASED fault-current levels due to load density growth and a greater number of network interconnections in distribution networks are common. The need to replace existing switchgear and their continuous upgrade as a result of increasing fault levels impose high costs for the utilities and their customers. In such a situation, the role of a fault-current limiter (FCL) is to ensure that the fault-current level is kept below the ratings of the existing switchgear, thus reducing or eliminating the costs involved in their upgrade. The limits on fault levels at electrical substations in New South Wales, Australia, are governed by guidelines recommended in [1], and there is a need to investigate how these limits can be achieved with the best possible solution, especially with the aid of superconducting FCLs.

There is renewed interest in superconducting FCLs due to the advantages offered by high-temperature superconductors (HTS) using liquid nitrogen over their low-temperature counterparts. This predominantly arises from an order of magnitude of savings in cryogenic equipment costs [2], and a reduction in operational costs by a factor of up to 100 [3]. Liquid nitrogen systems are also less complex compared to liquid helium systems.

Superconducting FCLs that have been examined in the past fall into two major categories: quench and nonquench types [4]. Quench-type FCLs rely on a fault current changing the effectively zero impedance of a superconductor during normal operation of the power system by quenching the superconductor, causing a rapid increase in its impedance. Quench-type FCLs suffer from operational difficulties caused by their slower fault response and recovery times. They also require additional equipment to prevent the burnout of the superconductor and cryogenics during a fault. In addition, the design of FCLs relying on power electronics is overly complex, and they have inherent reliability problems.

Manuscript received January 3, 2005; revised March 20, 2005. This work was supported in part by Metal Manufactures Ltd. and in part by the Australian Strategic Technology Program of the Electricity Supply Association of Australia. Paper no. TPWRD-00634-2004.

S. B. Abbott, D. A. Robinson, S. Perera, and C. J. Hawley are with the School of Electrical, Computer and Telecommunications Engineering, University of Wollongong, Wollongong NSW 2522, Australia (e-mail: duane@uow.edu.au).

F. A. Darmann and T. P. Beales are with Australian Superconductors, Port Kembla, NSW 2505, Australia (e-mail: tbeales@kembla.com.au).

Digital Object Identifier 10.1109/TPWRD.2005.859300

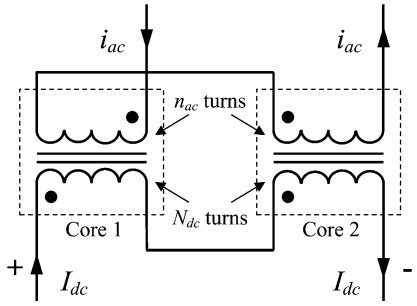

Fig. 1. Basic configuration of a saturable core-type FCL.

HTS saturable core-type FCLs provide superior properties for application in medium-voltage (MV) distribution systems. This is mainly due to the rapid, multishot ability, providing compatibility with reclosers, which clear more than 80% of overhead line faults in distribution systems [5]. Much of the past work on nonquench-type FCLs is covered in [4] and [6]. In a nonquench-type FCL, the superconductor is always in its superconducting state and the fault-current limiting takes place as a result of a change in magnetic saturation caused by the ac fault current.

The prototype saturable magnetic core-type FCL considered in this study is constructed using HTS tapes [7]. The application of HTS tapes in nonquench-type FCLs is most desirable from commercial and operational viewpoints: they are the most robust, practicable, and reliable forms available compared to other HTS forms. A description of the design principles applied to an HTS saturable core-type FCL is provided. Although specific to the presented scenarios, the design parameters of the FCL could be easily adjusted to suit various substation configurations. The concepts behind development of a time-domain model for the FCL are also presented, followed by simulation results in relation to the operation of the FCL for typical medium-voltage (MV) distribution substation applications.

II. Design Principles of Saturable Core-Type FCLs

A. Configuration of the FCL and Its Principle of Operation

The basics of saturable core-type FCLs are documented in several papers [3], [8]–[10] of which the essential features of a single-phase device are illustrated in Fig. 1. Two magnetic cores are required to cater for each half cycle of the ac fault current.

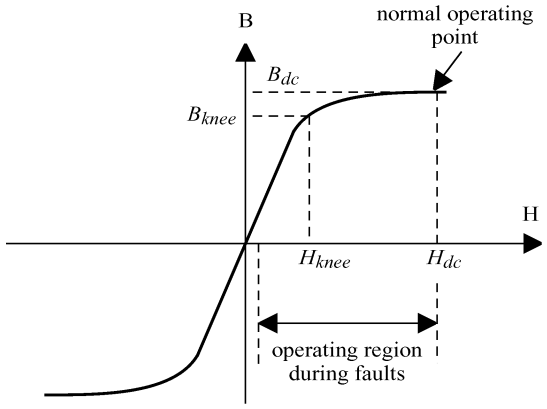

Fig. 2. Operating region of the saturable core-type FCL.

Each core carries a coil in which the ac line current $(i_{\rm ac})$ flows. An HTS coil carrying a dc bias current $(I_{\rm dc})$ is also wound on each core as illustrated in Fig. 1, where the dc bias current is common to both coils. The dc bias current saturates the iron core such that the inductance seen by the ac current during nonfault operation is negligible.

The magnetomotive force (MMF) produced by the superconducting dc winding is given by

$$N_{\rm dc}I_{\rm dc} = 2(2W + 2h)H_{\rm dc} \tag{1}$$

where $N_{\rm dc}$ is the number of turns in the dc winding, $I_{\rm dc}$ is the current in the dc winding, W is the average core width, h is the average core height, and $H_{\rm dc}$ is the magnetic field intensity due to the dc current. For the simulation model, the dc bias current is assumed constant. Practically, the ac fault current will have an effect on the dc bias current and needs to be considered in the design of the controlling power electronics.

The FCL inductance under normal power system conditions needs to be as small as possible. Therefore, the normal operating point is selected such that $H_{\rm dc} \gg H_{\rm knee}$, where $H_{\rm knee}$ is the saturation knee point indicated in Fig. 2.

When a fault current $(i_{\rm ac})$ flows through the ac winding, each core is alternatively taken out of saturation in each half cycle of $i_{\rm ac}$ as a result of the relatively large MMF caused by the fault current. To ensure that the FCL offers a large inductance during a fault, the MMF cancelation in each core should be such that

$$(H_{\rm dc} + H_{\rm knee})l \geq n_{\rm ac}I_F \geq (H_{\rm dc} - H_{\rm knee})l \tag{2}$$

where $H_{\rm dc} \gg H_{\rm knee}$, l is the length of the flux path around the core, $n_{\rm ac}$ is the number of turns in the ac winding, and I_F is the peak value of the fault current at which the FCL is designed to operate.

The conceptual design of the single-phase configuration has been extended to develop a three-phase FCL, where a single dc winding is used to control all ac phases. The design is innovative in that only one superconducting coil is used for all six of the magnetic cores. The three-phase design has been patented by Australian Superconductors [11].

III. Development of the FCL Simulation Model

A. Mathematical Model of the FCL

The slope of the nonlinear steel characteristics that is required to evaluate the terminal inductance of the FCL can be fitted by a curve of the form

$$\frac{dB}{dH} = e^a H^c e^{\frac{b}{H}} \tag{3}$$

where a, b, and c are constants representing the magnetizing properties of the steel core laminations. To determine the terminal inductance of the FCL, the nonlinear B–H characteristics of the laminated steel core for this model were represented within the 0–30 000-A/m region.

Based on (3), the per phase inductance L of the FCL due to the core flux alone (i.e., ignoring leakage flux) as a function of H is given by

$$L = \frac{An_{\rm ac}^2}{l}\frac{dB}{dH} \tag{4}$$

where A is the iron core cross-sectional area. Determination of the net magnetic field intensity H in the core is achieved by combining the effects of both the dc and ac fields

$$H = \frac{N_{\rm dc}I_{\rm dc} \pm n_{\rm ac}i_{\rm ac}}{l}. \tag{5}$$

As illustrated in Fig. 1, there are two cores per phase; thus, consideration of the dc and ac fields adding and subtracting is required and has been incorporated into the model.

B. Model Implementation in PSCAD/EMTDC

PSCAD/EMTDC [12] simulation studies were undertaken as a design verification tool and to examine the behavior of saturable core-type FCLs in relation to MV distribution substation applications.

The inductance associated with each phase of the FCL was included in the simulations as an externally controlled element, as illustrated in Fig. 3.

As shown in Fig. 3, the measured line current (i.e., $i_{\rm ac}$) is used to establish the variable FCL inductance in relation to each individual phase, and the remaining inputs ($N_{\rm dc}, I_{\rm dc}, a, b, c, n_{\rm ac}, A$ and l), governing the physical parameters of the windings and the core, are common to all of the FCL inductance calculations. In the PSCAD/EMTDC model, the FCL can be taken out of the simulation using the switched control element shown. Within PSCAD/EMTDC, the types of faults and the time of application can be easily controlled using the standard blocks.

Comparison of the PSCAD/EMTDC FCL model with actual measurements of the single-phase prototype FCL developed by Australian Superconductors [7] is illustrated in Fig. 4 for steady-state fault current, demonstrating reasonable agreement. The differences between simulation and measurements are due to the approximations involved in developing (3)–(5).

IV. Application Studies

Although several examples of substations were considered for the feasibility study, only one representative substation was chosen for simulation purposes and modeled in PSCAD/

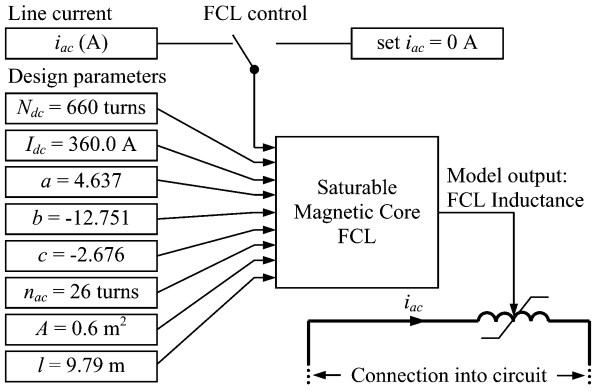

Fig. 3. PSCAD/EMTDC model setup for the calculation of the FCL inductance of each phase.

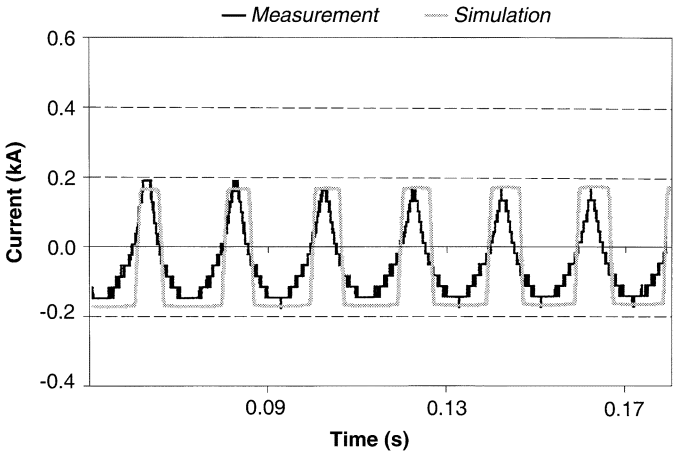

Fig. 4. Comparison of PSCAD/EMTDC model and prototype FCL measurements for steady-state fault current [7].

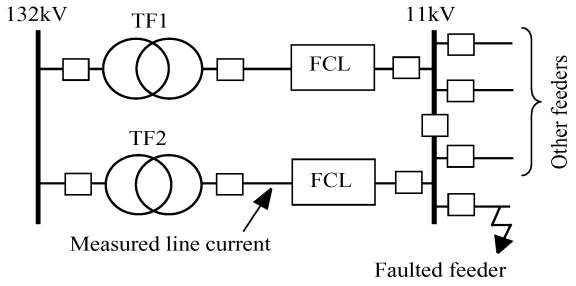

Fig. 5. Substation arrangement 1 with two FCLs in series with HV/MV transformers.

EMTDC. Two different implementations of the FCL in the substation were examined.

A. Initial Considerations

The first of the implementations is illustrated in Fig. 5, which shows two 45-MVA, 132/11-kV transformers connected to a common busbar supplying a mixture of several domestic and industrial feeders. The 11-kV busbar normally operates as a split-bus system in order to keep the fault-current level under control. The operation of these two transformers in parallel without the inclusion of any fault-current limiting results in a fault level of 272 MVA (i.e., $I_{\rm SC} = 14.3$ kA) for a three-phase line-to-ground fault on the 11-kV busbar. The stipulated regulations [1] require this level to be below 250 MVA ($I_{\rm SC} = 13.1$ kA).

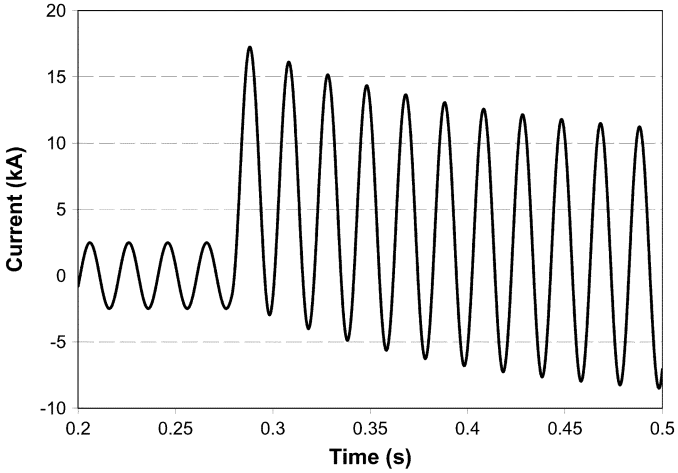

Fig. 6. Fault current on a transformer secondary without an FCL.

Practically, space and other issues had to be given due to consideration for the configuration in Fig. 5. Each FCL was designed to fit into a space of approximately $2.2 \times 2.2 \times 2.5$ m^3, incorporating existing 11-kV substation cables. Full details of the proposed design are provided in [7]. Provisions were also included to isolate the FCL. Each FCL was designed to be fitted with a range of sensors to monitor the liquid nitrogen, cooling system, and electrical supply to the FCL.

B. Simulation Results (Substation Arrangement 1)

All faults in the presented simulations were programmed to occur at $t = 0.28$ s. Fig. 6 shows the line current observed on the secondary of either of the transformers during a three-phase fault for the system of Fig. 5, without any external fault-current limiting.

The transient and steady-state performance of the FCL is very much dependent on the parameters $n_{\rm ac}, N_{\rm dc}, I_{\rm dc}, l$, and A. Hence, several designs can be examined to meet different criteria quite easily with the help of the simulations.

The FCLs can be designed to limit either the peak value of the initial transient fault current or its steady-state value. One criterion that can be used is to reduce the fault level for a three-phase-bolted ground fault on the 11-kV busbar to meet the 250-MVA regulation [1]. Fig. 7 shows the FCL inductance and the prefault and postfault line current waveforms for one of the transformer secondaries for a worst-case fault occurring at a voltage zero crossing on one of the phases.

As the ac line current changes, it is possible to have the MMF due to the ac line current completely counteracting the dc MMF, leading to a situation where the flux density is zero. At this point, based on the approach taken in modeling, the dynamic impedance as given by (3)–(5), the dynamic inductance is equal to zero. This behavior is evident from a close up view of the first few peaks of the line current, as illustrated in Fig. 8.

In practice, the total inductance is never equal to zero, as the leakage inductance of the ac winding is finite. Although the ac line current seems to be clipped, a close-up view would reveal that there are minute changes in the current resulting from the

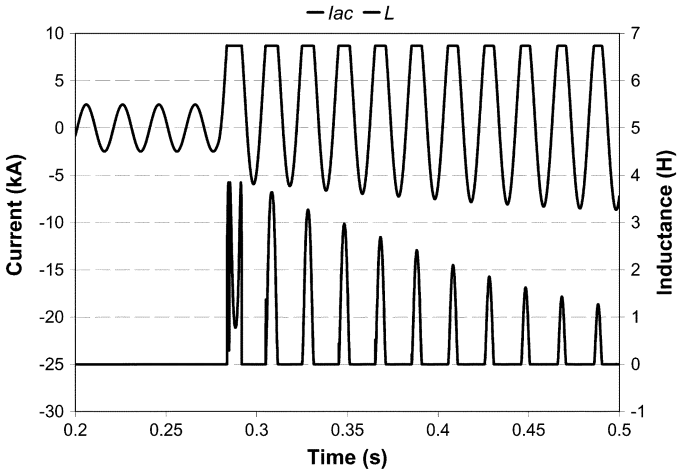

Fig. 7. Change in fault current and FCL inductance with time ($N_{\rm dc} = 580$ turns, $I_{\rm dc} = 360$ A, $n_{\rm ac} = 24$ turns).

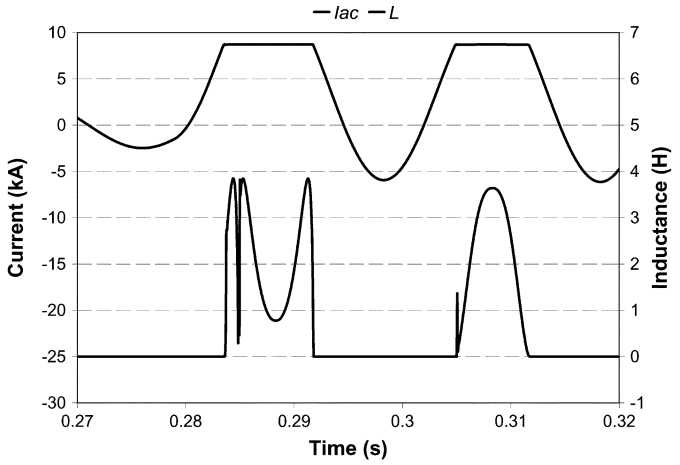

Fig. 8. Increased time step resolution view of a change in fault current and FCL inductance with time ($N_{\rm dc} = 580$ turns, $I_{\rm dc} = 360$ A, $n_{\rm ac} = 24$ turns).

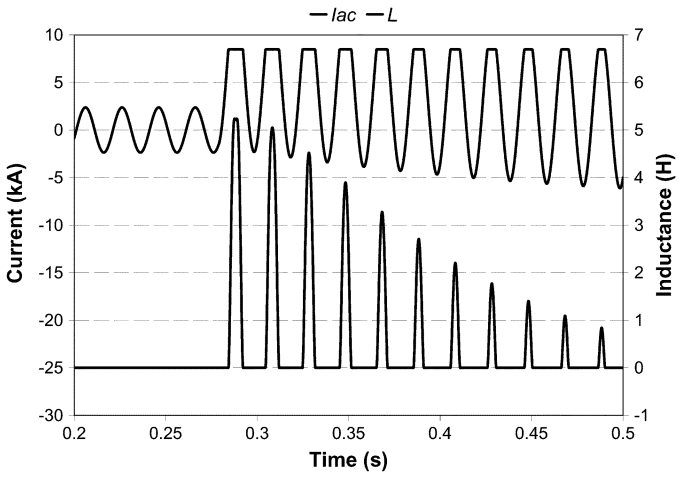

Fig. 9. Change in fault current and FCL inductance with time for increased $n_{\rm ac}$ and $N_{\rm dc}$ ($N_{\rm dc} = 660$ turns, $I_{\rm dc} = 360$ A, $n_{\rm ac} = 28$ turns).

change in the inductance. As this behavior is influenced by the leakage inductance of the ac coil, the finite per phase leakage inductance (0.7 mH) was included in the mathematical model for subsequent simulations.

Fig. 9 illustrates the behavior of the FCL system with an increased number of turns in both ac and dc windings together

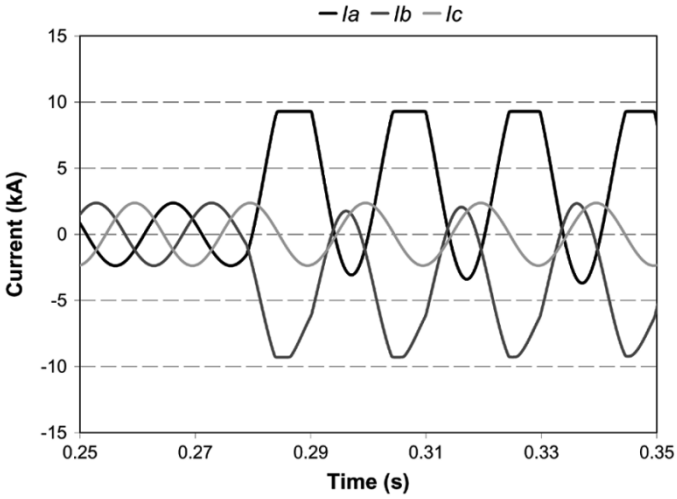

Fig. 10. Three-phase fault current with time for a line–line fault ($N_{\rm dc} = 580$ turns, $I_{\rm dc} = 385$ A, $n_{\rm ac} = 24$ turns).

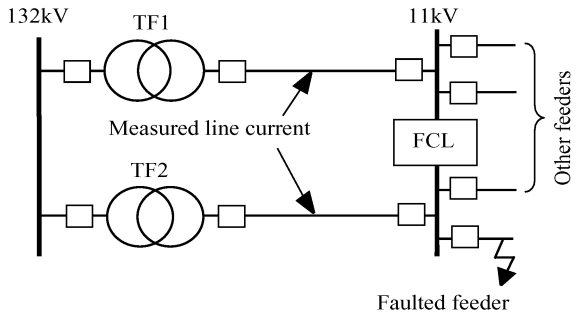

Fig. 11. Substation arrangement 2 with a single FCL on split bus.

with inclusion of the leakage inductance. As can be seen, the fault current is limited to an approximate 8.5 kA peak, which meets the fault level regulations. The corresponding maximum inductance of the FCL per phase is 5.22 H.

The square wave clipping operation of the ac current during fault-current limiting can lead to significant current harmonics. Simulations have shown that resonance caused by these harmonics due to system capacitance is unlikely. More practically, the actual waveforms are closer to a modified sinusoidal shape and not a full square wave, as indicated by Fig. 4 and, thus, will contain less higher order harmonics and further reduce the likelihood of low-frequency resonance.

Another criterion in the design of the FCL was to limit the first peak of the fault current on the 11-kV busbar to a maximum of 18.6 kA, or 9.3 kA peak per transformer secondary. Such a reduction in the fault current by the FCL is achieved using $N_{\rm dc} = 580$ A, $I_{\rm dc} = 385$ A, and $n_{\rm ac} = 24$ turns, corresponding to a maximum inductance of the FCL of 3.85 H per phase.

Other fault types were also considered including single line-to-ground and line–line faults. Fig. 10 shows the transformer secondary currents for a line–line fault on the 11-kV busbar, respectively. As expected, the line current is clipped at 9.3 kA.

C. Simulation Results (Substation Arrangement 2)

An alternative arrangement for the installation of an FCL in a substation is shown in Fig. 11. This example only requires a single FCL located on the MV busbar, joining the two busbars that would normally be in a split-bus configuration.

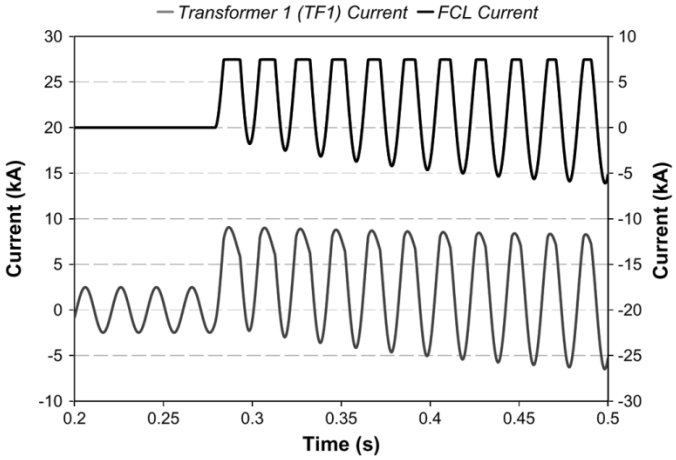

Fig. 12. Substation arrangement 2 transformer currents during fault ($N_{\rm dc} = 560$ turns, $I_{\rm dc} = 400$ A, $n_{\rm ac} = 30$ turns).

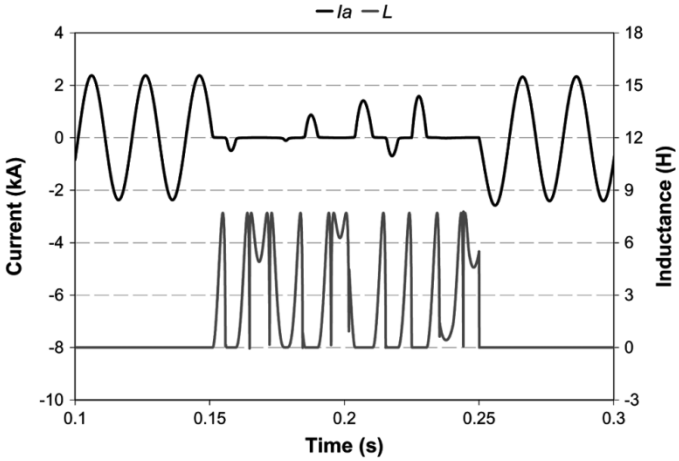

Fig. 13. Transformer current and FCL inductance during loss of dc bias current to both FCLs in substation arrangement 1.

In this case, when a fault occurs on the busbar section closer to transformer 2, only the current from transformer 1 will be limited. As such, to obtain the same reduction in fault level, and to bring the network in line with regulations, the FCL is required to clamp the current from transformer 1 at a smaller magnitude than that in the substation arrangement 1 example. It was found that the current flowing through the FCL from transformer 1 had to be limited to 7.5 kA peak. This could be achieved by modifying the FCL design by increasing the value of $I_{\rm dc}$ and $n_{\rm ac}$.

The currents passing through the FCL and transformer 1 during a fault at the location shown are illustrated in Fig. 12. The FCL waveform is as per Fig. 9; however, the peak is now limited to 7.5 kA. These waveforms result in an 11-kV bus total fault level of 250 MVA, as stipulated by the regulations. Transformer 1 current waveform is rounded at the peak maximum because, at this point, current is also flowing to the load as the FCL impedance limits the flow of current to the fault. By limiting the fault current from transformer 1, the sag performance at the transformer 1 busbar can be improved for faults further along the faulted feeder.

As seen in Fig. 12, a small amount of distortion is present on the current waveform of transformer 1. The level of distortion is minimal and is unlikely to affect other loads before the circuit breakers (CBs) or reclosers clear the fault.

D. Other FCL Applications

In larger sized distribution systems, it may be feasible to install HTS saturable core-type FCLs between the substation busbar and an MV feeder. The design of such an FCL can be based on reducing fault current to customers with insufficient switchgear rating, or to provide improved sag performance to customers connected to other feeders. Overlap with reclosers and ensuring fault levels remains detectable by protection devices and needs to be carefully considered for such applications.

FCL devices also have applications for interconnecting distribution systems and at the connection points of large distributed generators. This allows systems to be reconfigured to improve reliability or protect customers from damaging sags and high fault levels. The behavior of HTS saturated core-type FCLs for such applications would be nearly identical to that demonstrated in this paper.

E. HTS Saturable Core-Type FCL Protection Issues

Reliability of saturable magnetic core-type FCLs is superior to other types of superconducting FCLs due to simplicity of components and reduced cryogenic requirements. The cryogenics and dc current supply remain the critical components for FCL operation and reliability.

Loss of dc bias current will cause some disruption to system operation due to the resulting change in FCL impedance. Fig. 13 illustrates the impedance changes of the FCL during a loss of dc bias current to both FCLs for the configuration of Substation Arrangement 1. The dc bias current is removed from $t = 0.15$ to $t = 0.25$ s, and a constant impedance load has been assumed. Fast acting bypass switches and backup protection are required for MV distribution system applications and are included in the proposed design for substation arrangement 1 [7].

V. Conclusion

The design principles of a prototype HTS saturable magnetic core-type FCL have been elucidated, and case studies in relation to typical MV distribution substations have been examined.

The important parameters that govern the behavior of an FCL were chosen to meet the physical constraints of the particular substation under consideration, performance of the system, and the regulatory requirements in force.

A mathematical model describing the FCL operation that allows modification to the important design parameters has been presented. Time-domain simulations were carried out to illustrate the behavior of such FCLs under fault conditions.

Further development of the single-phase prototype HTS saturable magnetic core-type FCL is required to enable production of a functional three-phase FCL unit suitable for practical MV substation applications.

References

[1] Elect. Assoc. NSW, *NSW Service and Installation Rules*, 2nd ed., Mar. 1999, vol. S7.5.4, p. 160.

[2] L. Salasoo *et al.*, "Comparison of superconducting fault current limiter concepts in electric utility applications," *IEEE Trans. Appl. Superconduct.*, vol. 5, no. 2, pp. 1079–1082, Jun. 1995.

[3] F. Mumford, "Superconducting fault current limiters," in *Inst. Elect. Eng. Colloq.*, Jun. 1995, pp. 6/1–6/7.

[4] Y. Jiang *et al.*, "Comparison of superconducting fault current limiter in power system," in *Proc. IEEE Power Eng. Soc. Meeting*, vol. 1, 2001, pp. 43–47.
[5] J. D. Glover and M. S. Sarma, *Power System Analysis and Design*, 3rd ed. Pacific Grove, CA, 2002, pp. 466–469.
[6] Y. C. Tan and P. D. Evans, "Quenching behavior of superconductors in an inductive fault current limiter," *IEEE Trans. Appl. Supercond.*, vol. 11, no. 1, pp. 2495–2498, Mar. 2001.
[7] F. Darmann and T. Beales, "New fault current limiters for utility substations—Design, analysis, construction, and testing," in *Proc. TechCon Asia–Pacific Conf.*, Sydney, NSW, Australia, 2003.
[8] A. T. Rowley, "Superconducting fault current limiters," in *Inst. Elect. Eng. Colloq.*, Dec. 1995, pp. 10/1–10/3.
[9] B. P. Raju, K. C. Parton, and T. C. Bartram, "Fault current limiting reactor with superconducting dc bias winding," CIGRE, Sep. 1982. Paper 23–03.
[10] J. X. Jin *et al.*, "Electrical application of high Tc superconducting saturable core fault current limiter," *IEEE Trans. Appl. Supercond.*, vol. 7, no. 2, pp. 1009–1012, Jun. 1997.
[11] F. A. Darmann and T. P. Beales, "Superconducting Fault Current Limiter," Australian Superconductors Patent 04 038 817, May 6, 2004.
[12] *Manitoba HVDC Research Centre, Inc.*. PSCAD/EMTDC, Version 4.1.0.

S. B. Abbott (M'03) received the B.E. degree (Hons.) in electrical engineering from the University of Wollongong, Wollongong, NSW, Australia. He completed his final year thesis on the applications of superconductor FCLs.

Currently, he is an Electrical Engineer with Energy Australia, working in the area of demand management and network planning.

D. A. Robinson received the B.E. (Hons.) degree and Ph.D. degree in harmonics management from the University of Wollongong, Wollongong, NSW, Australia.

Currently, he is a Senior Lecturer at the University of Wollongong and has been with BHP Steel.

Dr. Robinson is a member of the Integral Energy Power Quality and Reliability Centre.

S. Perera (M'95) received the B.Sc. degree in power from the University of Moratuwa, Sri Lanka, and the M.Eng.Sc. and Ph.D. degrees from the University of New South Wales, Sydney, Australia.

He was a Lecturer with the University of Moratuwa. Currently, he is an Associate Professor with the University of Wollongong, Wollongong, NSW, Australia. He is the Technical Director of the Integral Energy Power Quality and Reliability Centre at the University of Wollongong.

F. A. Darmann received the Ph.D. degree from the University of Wollongong, Wollongong, NSW, Australia.

Currently, he is an Electrical Engineer with the Australian Nuclear Science and Technology Organization, Sydney, Australia.

C. J. Hawley received the B.E. (Hons.) degree in telecom engineering from the University of Wollongong, Wollongong, NSW, Australia, where he is currently pursuing the Ph.D. degree in the area of superconductor energy storage in conjunction with Australian Superconductors, Port Krembla, NSW, Australia.

He is a Research Engineer with the University of Wollongong.

T. P. Beales is Manager of the Australian Superconductors and Visiting Professor at the Institute of Superconducting and Electronic Materials, University of Wollongong, Wollongong, NSW, Australia.